

# Proof-of-principle experimental demonstration of quantum gate verification

Maolin Luo,<sup>1</sup> Xiaoqian Zhang,<sup>1,\*</sup> and Xiaoqi Zhou<sup>1,†</sup>

<sup>1</sup>*School of Physics and State Key Laboratory of Optoelectronic Materials and Technologies, Sun Yat-sen University, Guangzhou 510000, China*  
(Dated: July 29, 2021)

To employ a quantum device, the performance of the quantum gates in the device needs to be evaluated first. Since the dimensionality of a quantum gate grows exponentially with the number of qubits, evaluating the performance of a quantum gate is a challenging task. Recently, a scheme called quantum gate verification (QGV) has been proposed, which can verify quantum gates with near-optimal efficiency. In this work, we implement a proof-of-principle optical experiment to demonstrate this QGV scheme. We show that for a single-qubit quantum gate, only  $\sim 400$  samples are needed to confirm the fidelity of the quantum gate to be at least 97% with a 99% confidence level using the QGV method, while at least  $\sim 5000$  samples are needed to achieve the same result using the standard quantum process tomography method. The QGV method validated by this work has the potential to be widely used for the evaluation of quantum devices in various quantum information applications.

Quantum information technology can greatly improve the speed of computation, the security of communication, and the precision of measurement. To make good use of quantum information technology, it is first necessary to characterize quantum devices to evaluate their performance. The standard method for characterizing quantum devices is quantum process tomography (QPT) [1–7], which allows complete reconstruction of the quantum process of the device, but its resource overhead grows exponentially with the size of the system, making it impractical when the system is large. However, for most applications, the complete information of the quantum device is not needed, but only the fidelity of the evaluated device compared to a perfect device. For this reason, methods such as direct fidelity estimation [8] and randomized benchmarking [9–14] have been proposed to estimate the fidelity of quantum gates. Although these methods improve the efficiency of the verification of quantum gates, they require a very large number of experimental settings and are not optimal in terms of the scaling behavior between the predicted upper limit of the infidelity  $\epsilon$  and the number of samples  $N$ .

Recently, a quantum gate verification (QGV) [15–17] scheme developed from the quantum state verification (QSV) [18–32] scheme has been proposed. This scheme allows gate verification of a variety of quantum gates with near-optimal efficiency using only local state preparation and local measurements. In this Letter, we implement a proof-of-principle optical experiment to demonstrate this QGV scheme. We randomly selected two arbitrary single-qubit gates and performed QGV on them. It has been shown that only  $\sim 400$  samples are needed to confirm the fidelity of the quantum gate to be at least 97% with a 99% confidence level, while at least  $\sim 5000$  samples are needed to achieve the same result using the QPT method. In addition, the QPT method requires 18 experimental settings compared to the QGV method which only requires 6 experimental settings. Our results demonstrate that quantum gates can be efficiently verified using the QGV method.

*Theoretical framework for quantum-gate verification.* — We first briefly review how to transform a QGV problem into

a QSV problem [15–17]. As shown in Fig. 1(a),  $k$  qubits of a  $2k$ -qubit quantum state  $\rho$  are passed through a quantum process  $\Lambda_{ideal}$  thereby obtaining an output state  $\rho_{ideal}$ . If no other quantum process except  $\Lambda_{ideal}$  can convert  $\rho$  to  $\rho_{ideal}$  in this way, then the quantum process  $\Lambda_{ideal}$  corresponds exactly to the quantum state  $\rho_{ideal}$ . Therefore, the problem of verifying whether a quantum process  $\Lambda_{device}$  is equal to  $\Lambda_{ideal}$  is transformed into the problem of verifying whether the output state  $\rho_{device}$  obtained from the quantum state  $\rho$  through the quantum process  $\Lambda_{device}$  is equal to  $\rho_{ideal}$ .

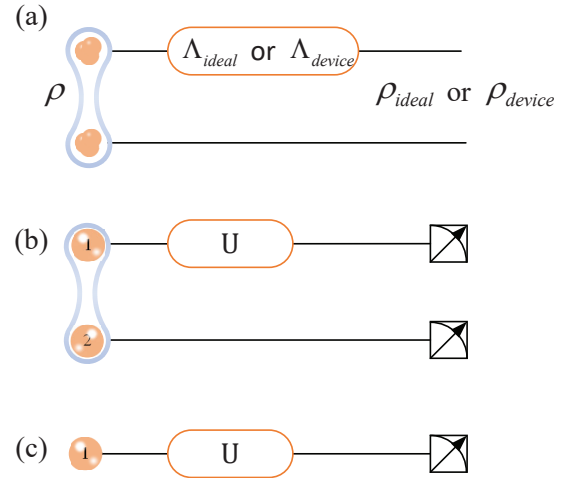


FIG. 1. (Color online) The schematic of quantum gate verification. (a) Transformation of quantum gate verification problem to quantum state verification problem. By using the entangled probing state  $\rho$ , the problem of whether the quantum process  $\Lambda_{device}$  is equal to  $\Lambda_{ideal}$  is transformed into the problem of whether the output quantum state  $\rho_{device}$  is equal to  $\rho_{ideal}$ . (b) The quantum gate verification of a single-qubit unitary  $U$  using a two-qubit entangled probing state. (c) The quantum gate verification of a single-qubit unitary  $U$  using only single-qubit probing states.

In the following, we take an arbitrary single-qubit gate  $U$  as an example to illustrate the method of QGV in detail. As shown in Fig. 1(b), the two-qubit state  $\phi$  is used as the input

\* zhangxq67@mail.sysu.edu.cn

† zhouxq8@mail.sysu.edu.cn

state, where

$$\phi = \frac{1}{2}(|0\rangle_1|0\rangle_2 + |1\rangle_1|1\rangle_2). \quad (1)$$

After passing qubit 1 through a quantum process  $\Lambda_{device}$ , the output two-qubit state  $\phi_{\Lambda_{device}}$  would be equal to  $\phi_U$  if  $\Lambda_{device}$  is equal to the  $U$  operation, in which

$$\phi_U = \frac{1}{2}(U|0\rangle_1 \otimes |0\rangle_2 + U|1\rangle_1 \otimes |1\rangle_2). \quad (2)$$

The efficient strategy for verifying whether  $\phi_{\Lambda_{device}}$  is equal to  $\phi_U$  can be defined by the operator  $\Omega_{\phi_U} = \frac{1}{3}(P_{(UXU^\dagger)_1 X_2}^+ + P_{(UYU^\dagger)_1 Y_2}^- + P_{(UZU^\dagger)_1 Z_2}^+)$ . It can be realized by randomly choosing one of the three bases  $(UXU^\dagger)_1 X_2$ ,  $(UYU^\dagger)_1 Y_2$  and  $(UZU^\dagger)_1 Z_2$  for measurement. When the measurement basis is  $(UXU^\dagger)_1 X_2$  or  $(UZU^\dagger)_1 Z_2$ , the measurement result +1 is taken as a pass, and when the measurement basis is  $(UYU^\dagger)_1 Y_2$ , the measurement result -1 is taken as a pass. Suppose we have  $N$  copies of  $\phi_{\Lambda_{device}}$ , the verification is passed only when all  $N$  measurement outcomes are passed, at which point it can be claimed that the fidelity of  $\phi_{\Lambda_{device}}$  with respect to  $\phi_U$  is at least  $1 - \epsilon$ , with  $1 - \delta$  confidence, where

$$\delta \leq e^{-\epsilon N \nu}, \quad (3)$$

in which  $\nu$  is the difference between the largest and the second largest eigenvalues of  $\Omega_{\phi_U}$ .

The original scheme above requires all measurement outcomes to be passed, which is difficult to achieve in practice, so we will use a modified version of the scheme [31] that allows for failed outcomes. If among  $N$  measurement outcomes,  $M$  are passed, then when  $\epsilon \geq \frac{1-M/N}{\nu}$ , it can be claimed that the fidelity is at least  $1 - \epsilon$ , with  $1 - \delta$  confidence, where

$$\delta \leq e^{-D(\frac{M}{N} || 1-\epsilon)N}, \quad (4)$$

with

$$D(x||y) = x \log_2 \left( \frac{x}{y} \right) + (1-x) \log_2 \left( \frac{1-x}{1-y} \right).$$

By analyzing the above scheme, it can be found that the measurements on qubit 2 can occur before qubit 1 pass through the quantum gate, which means the scheme of preparing a two-qubit entangled state as the input state can be transformed into a scheme of preparing some single-qubit states as the input state. Taking the  $(UZU^\dagger)_1 Z_2$  measurement setting as an example, measuring qubits 1 and 2 of the state  $|\phi\rangle$  first is equivalent to preparing a single-qubit state  $|0\rangle$  or  $|1\rangle$  randomly with equal probability, letting it pass through the quantum gate, and then performing a  $UZU^\dagger$  measurement on it. Therefore, the verification scheme for the single-qubit gate becomes — prepare one of the following six single-qubit quantum states  $|0\rangle$ ,  $|1\rangle$ ,  $|+\rangle$ ,  $|-\rangle$ ,  $|+i\rangle$  and  $| -i\rangle$  randomly with equal probability and let it pass through the quantum gate and then measure it at a certain basis, where  $|\pm\rangle = \frac{1}{\sqrt{2}}(|0\rangle \pm |1\rangle)$  and  $|\pm i\rangle = \frac{1}{\sqrt{2}}(|0\rangle \pm i|1\rangle)$ . If the initial state is  $|0\rangle$  ( $|+\rangle$  /  $| -i\rangle$ ), then it is measured at  $UZU^\dagger$  ( $UXU^\dagger$  /  $UYU^\dagger$ ) basis and the verification passes with outcome +1; if the initial state is

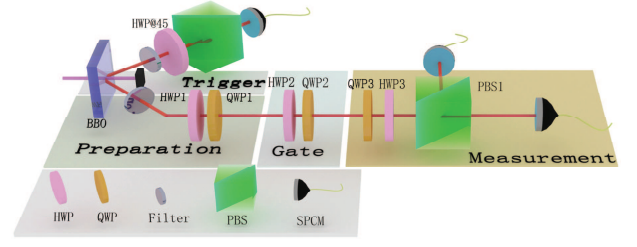


FIG. 2. (Color online) Experimental Setup. An ultraviolet laser is focused on a type-II beta-barium borate (BBO) crystal and produces a photon pair. After the triggering of photon 2, photon 1 is prepared at the desired state by tuning HWP1 and QWP1. After passing through the single-qubit gate, which is realized by HWP2 and QWP2, photon 1 is measured by the device (QWP3, HWP3, PBS1 and the two SPCMs) at the desired basis. HWP: half-wave plate; QWP: quarter-wave plate; PBS: Polarization Beamsplitter; SPCM: Single-Photon Counting Module.

$|1\rangle$  ( $|-\rangle$  /  $|+i\rangle$ ), then it is measured at  $UZU^\dagger$  ( $UXU^\dagger$  /  $UYU^\dagger$ ) basis and the verification passes with outcome -1.

*Experimental setup.* —The experimental setup to implement the single-qubit gate verification is shown in Fig. 2. An ultraviolet laser with a central wavelength of 405 nm is focused on a type-II beta-barium-borate (BBO) crystal to generate a photon pair  $|H\rangle_1|V\rangle_2$ , where H and V denote horizontal and vertical polarizations respectively. After the triggering of photon 2, photon 1 is prepared at the desired state via the half-wave plate HWP1 and the quarter-wave plate QWP1 as the input state for the verification of the quantum gate, which is realized by HWP2 and QWP2. After passing through the quantum gate, the output quantum state is measured by the device (QWP3, HWP3, the polarization beamsplitter PBS1 and the single-photon counting modules SPCMs) at the desired measurement basis.

*Results.* —We choose two general single-qubit gates  $U_a$  and  $U_b$  for demonstrating the scheme of QGV, where

$$U_a = \begin{pmatrix} -0.7071 + 0.3536i & 0.6124i \\ 0.6124i & -0.7071 - 0.3536i \end{pmatrix}, \quad (5)$$

$$U_b = \begin{pmatrix} -0.1228 - 0.2418i & -0.6964 + 0.6645i \\ 0.6964 + 0.6645i & -0.1228 + 0.2418i \end{pmatrix}.$$

To verify  $U_a$  ( $U_b$ ) gate, we prepare  $|H\rangle$ ,  $|V\rangle$ ,  $|D\rangle$ ,  $|A\rangle$ ,  $|R\rangle$  and  $|L\rangle$  randomly with equal probability as the input state, in which  $|D/A\rangle = \frac{1}{\sqrt{2}}(|H\rangle \pm |V\rangle)$  and  $|R/L\rangle = \frac{1}{\sqrt{2}}(|H\rangle \pm i|V\rangle)$ , and measure the output state on the measurement basis  $\chi_{a1}^+/\chi_{a1}^-$  ( $\chi_{b1}^+/\chi_{b1}^-$ ) for the input states  $|H\rangle$  and  $|V\rangle$  or  $\chi_{a2}^+/\chi_{a2}^-$  ( $\chi_{b2}^+/\chi_{b2}^-$ ) for the input states  $|D\rangle$  and  $|A\rangle$  or  $\chi_{a3}^+/\chi_{a3}^-$  ( $\chi_{b3}^+/\chi_{b3}^-$ ) for the

input states  $|R\rangle$  and  $|L\rangle$ , where

$$\begin{aligned} \chi_{a_1}^+ &= \begin{pmatrix} -0.7071 + 0.3536i \\ 0.6124i \end{pmatrix}, \chi_{a_1}^- = \begin{pmatrix} 0.6124i \\ -0.7071 - 0.3536i \end{pmatrix}, \\ \chi_{a_2}^+ &= \begin{pmatrix} -0.5000 + 0.6830i \\ -0.5000 + 0.1830i \end{pmatrix}, \chi_{a_2}^- = \begin{pmatrix} -0.5000 - 0.1830i \\ 0.5000 + 0.6830i \end{pmatrix}, \\ \chi_{a_3}^+ &= \begin{pmatrix} -0.9330 + 0.2500i \\ 0.2500 - 0.0670i \end{pmatrix}, \chi_{a_3}^- = \begin{pmatrix} -0.0670 + 0.2500i \\ -0.2500 + 0.9330i \end{pmatrix}, \\ \chi_{b_1}^+ &= \begin{pmatrix} -0.1228 - 0.2418i \\ 0.6964 + 0.6645i \end{pmatrix}, \chi_{b_1}^- = \begin{pmatrix} -0.6964 + 0.6645i \\ -0.1228 + 0.2418i \end{pmatrix}, \\ \chi_{b_2}^+ &= \begin{pmatrix} -0.5792 + 0.2988i \\ 0.4056 + 0.6409i \end{pmatrix}, \chi_{b_2}^- = \begin{pmatrix} 0.4056 - 0.6409i \\ 0.5792 + 0.2988i \end{pmatrix}, \\ \chi_{b_3}^+ &= \begin{pmatrix} -0.5567 - 0.6634i \\ 0.3214 + 0.3830i \end{pmatrix}, \chi_{b_3}^- = \begin{pmatrix} 0.3830 + 0.3214i \\ 0.6634 + 0.5567i \end{pmatrix}. \end{aligned}$$

In order to show the advantages of the QGV method over the traditional QPT method, in addition to the gate verification of  $U_a$  and  $U_b$  with QGV, we also evaluated the infidelity of  $U_a$  and  $U_b$  with the QPT method (see APPENDIX A), and the relevant experimental results are shown in Fig. 3. For a given confidence level  $1 - \delta$ , the infidelity  $\epsilon$  decreases as the number of samples  $N$  increases, and the faster it decreases, the more effective the method is. It can be seen that for both  $U_a$  and  $U_b$ , QGV allows  $\epsilon$  to decrease faster with increasing  $N$  compared to QPT (the confidence level  $1 - \delta$  is set to 99%). For  $U_a$  ( $U_b$ ), the infidelity can be achieved down to 0.03 using the QSV method with only 365 (434) samples, while 6427 (4130) samples are required to achieve the same level of infidelity using the QPT method. To quantify the rate of decrease of  $\epsilon$  with  $N$ , the data are fitted in the interval  $N < 500$  using  $\epsilon \sim N^r$  [33–35], where  $r$  is the descent slope of the fitting line. For  $U_a$  ( $U_b$ ), while QPT's descent slope is just  $-0.58 \pm 0.07$  ( $-0.62 \pm 0.08$ ), QGV's descent slope is  $-0.92 \pm 0.02$  ( $-0.93 \pm 0.02$ ), which is quite close to the Heisenberg scaling value  $-1$ . Here QGV experiments are repeated 50 times and QPT experiments are repeated 15 times in order to calculate the error bar shown in Fig. 3. In terms of experimental settings, the QGV method is more efficient compared to the QPT method, where 6 experimental settings are used in the above experiments for QGV, while 18 experimental settings are used for QPT.

In addition to the gate verification of single-qubit gates, we also verify a two-qubit CNOT gate using the QGV method (see APPENDIX B). Although the fidelity of the implemented two-photon CNOT gate itself is not high enough for QGV to show an advantage over QPT in terms of the number of samples, QGV still shows a great advantage in terms of the number of experimental settings, with only 16 experimental settings required for QGV, compared to 324 experimental settings for QPT.

*Summary.*—We have experimentally demonstrated the QGV protocol that enables efficient verification of quantum gates. Our experimental results show that the evaluation of quantum gate infidelity can approach the Heisenberg scaling ( $1/N$ ) which greatly saves the resources needed to evaluate the fidelity of quantum gates compared to the standard QPT method. The QGV method validated by this work is expected

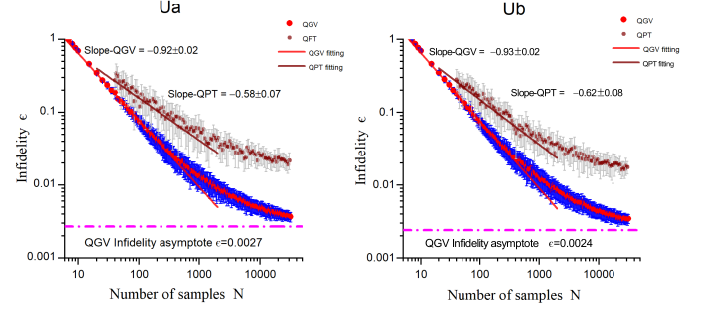


FIG. 3. (Color Online) Experimental results of QGV for  $U_a$  and  $U_b$ . The red dots correspond to the data of QGV and the brown dots correspond to the data of QPT. The red and brown lines are the fitted lines to the QGV and QPT data, respectively. Here the confidence level  $1 - \delta$  is set to 99%. The fitting interval is the interval with sample size  $N$  less than 500. The fitting formula is  $\epsilon \sim N^r$ , where  $\epsilon$  denotes the infidelity and  $r$  denotes the descent slope of the fitted line. For  $U_a$  ( $U_b$ ), while QPT's descent slope is just  $-0.58 \pm 0.07$  ( $-0.62 \pm 0.08$ ), QGV's descent slope is  $-0.92 \pm 0.02$  ( $-0.93 \pm 0.02$ ), which is quite close to the Heisenberg scaling value  $-1$ .

to be widely used for the evaluation of quantum devices and for various quantum information applications including quantum process discrimination [36], quantum channel quantification [37] and quantum entanglement detection [38].

This work was supported by the National Key Research and Development Program (2017YFA0305200), the Key Research and Development Program of Guangdong Province of China (2018B030329001 and 2018B030325001), the National Natural Science Foundation of China (Grant No. 61974168). X. Zhou acknowledges support from the National Young 1000 Talents Plan. X. Zhang acknowledges support from the National Natural Science Foundation of China (Grant No. 62005321).

## APPENDIX A: QUANTUM PROCESS TOMOGRAPHY OF THE $U_a$ AND $U_b$ GATES

To implement QPT on  $U_a$  and  $U_b$ , six probing states  $|H\rangle$ ,  $|V\rangle$ ,  $|D\rangle$ ,  $|A\rangle$ ,  $|R\rangle$  and  $|L\rangle$  and three measurement bases X, Y, and Z are used. The measured data are then processed using the maximum likelihood method to calculate the process matrices of  $U_a$  and  $U_b$ . The results are shown in Fig. 4, from which the fidelity of  $U_a$  ( $U_b$ ) can be calculated as  $0.9801 \pm 0.003$  ( $0.9829 \pm 0.003$ ).

## APPENDIX B: QUANTUM GATE VERIFICATION FOR THE TWO-QUBIT CNOT GATE

The experimental setup to implement the two-qubit CNOT gate verification is shown in Fig. 5. The same photon source as in Fig. 2 is used to obtain the two-photon state  $|H\rangle_1|V\rangle_2$ , which is then prepared to the desired two-qubit state via

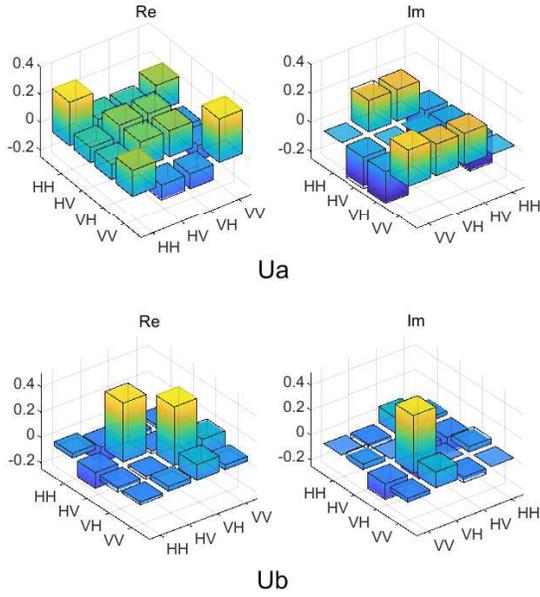


FIG. 4. (Color online) QPT results for  $U_a$  and  $U_b$ . Here “Re” and “Im” refer to the real and imaginary parts of the process matrices, respectively. The fidelity of  $U_a$  is  $0.9801 \pm 0.003$  and the fidelity of  $U_b$  is  $0.9829 \pm 0.003$ .

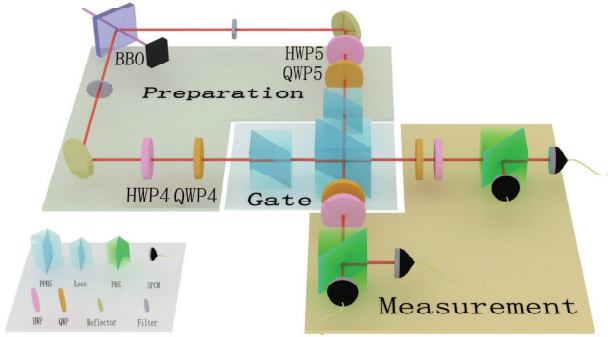


FIG. 5. (Color online) Experimental Setup for verifying the CNOT gate. An ultraviolet (UV) laser is focused on a type-II beta-barium borate (BBO) crystal and produces a photon pair. Photon 1 and Photon 2 are prepared at the desired state by tuning HWP4, QWP4, HWP5 and QWP5. After passing through the CNOT gate, which is constructed from three partial polarization beamsplitters (PPBS), photon 1 and photon 2 are then measured separately at the desired basis. HWP: half-wave plate; QWP: quarter-wave plate; PBS: Polarization Beamsplitter; SPCM: Single-Photon Counting Module.

HWP4, QWP4, HWP5 and QWP5 as the input state for verifying the CNOT gate. One of the following eight two-qubit

quantum states

$$\begin{aligned}
 \phi_{IZ}^+ &= \frac{I_1}{2} \otimes |0\rangle_2 \langle 0|, & \phi_{IZ}^- &= \frac{I_1}{2} \otimes |1\rangle_2 \langle 1|, \\
 \phi_{ZI}^+ &= |0\rangle_1 \langle 0| \otimes \frac{I_2}{2}, & \phi_{ZI}^- &= |1\rangle_1 \langle 1| \otimes \frac{I_2}{2}, \\
 \phi_{IX}^+ &= |+\rangle_1 \langle +| \otimes \frac{I_2}{2}, & \phi_{IX}^- &= |-\rangle_1 \langle -| \otimes \frac{I_2}{2}, \\
 \phi_{XI}^+ &= \frac{I_1}{2} \otimes |+\rangle_2 \langle +|, & \phi_{XI}^- &= \frac{I_1}{2} \otimes |-\rangle_2 \langle -|
 \end{aligned} \tag{6}$$

are prepared randomly with equal probability and then pass through the CNOT gate, which is constructed from three partial polarization beamsplitters (PPBS) reference [39]. After passing through the CNOT gate, photon 1 and photon 2 are then measured separately at the desired measurement basis. If the initial state is  $\phi_{IZ}^+$  ( $\phi_{ZI}^+$ ,  $\phi_{IX}^+$ ,  $\phi_{XI}^+$ ), then it is measured at ZZ (ZI, IX, XX) basis and the verification passes with outcome +1; if the initial state is  $\phi_{IZ}^-$  ( $\phi_{ZI}^-$ ,  $\phi_{IX}^-$ ,  $\phi_{XI}^-$ ), then it is measured at ZZ (ZI, IX, XX) basis and the verification passes with outcome -1.

The experimental results are shown in Fig. 6, which shows that the infidelity decreases  $\epsilon$  with the increase of the number of samples  $N$ . As the fidelity of the implemented two-photon CNOT gate is not high enough, which is  $\sim 87\%$  in our case, QGV cannot show an advantage over QPT in terms of the number of samples. However, QGV still shows a great advantage in terms of the number of experimental settings, with only 16 experimental settings required for QGV, compared to 324 experimental settings for QPT.

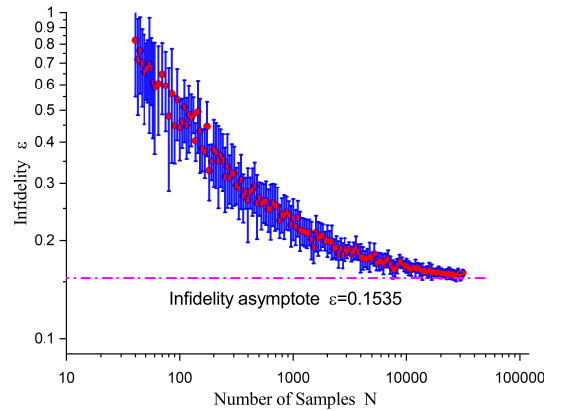


FIG. 6. (Color online) Experimental results of quantum gate verification for the two-qubit CNOT gate. The red dots correspond to the data of QGV. Here the confidence level  $1 - \delta$  is set to 99%.

[1] Y. Deville and A. Deville, Quantum process tomography with unknown single-preparation input states: Concepts and application to the qubit pair with internal exchange coupling. Phys.

Rev. A 101, 042332 (2020).

[2] H. P. Lo, T. Ikuta, N. Matsuda, T. Honjo, William J. Munro and H. Takesue. Quantum Process Tomography of a Controlled-

- Phase Gate for Time-Bin Qubits. *Phys. Rev. Appl.* 13, 034013 (2020).
- [3] Y. S. Teo, G. I. Struchalin, E. V. Kovlakov, D. Ahn, H. Jeong, S. S. Straupe, S. P. Kulik, G. Leuchs and L. L. Sánchez-Soto. Objective compressive quantum process tomography. *Phys. Rev. A* 101, 022334 (2020).
- [4] Z. H. Hou, J. F. Tang, C. Ferrie, G. Y. Xiang, C. F. Li and G. C. Guo. Experimental realization of self-guided quantum process tomography. *Phys. Rev. A* 101, 022317 (2020).
- [5] F. Bouchard, F. Hufnagel, D. Koutný, A. Abbas, A. Sit, K. Heshami, R. Fickler and E. Karimi. Quantum process tomography of a high-dimensional quantum communication channel. *Quantum* (2019).
- [6] Y. Gazit, H. K. Ng and J. Suzuki, Quantum process tomography via optimal design of experiments. *Phys. Rev. A* 100, 012350 (2019).
- [7] L. P. Thinh, P. Faist, J. Helsen, D. Elkouss and S. Wehner, Practical and reliable error bars for quantum process tomography. *Phys. Rev. A* 99, 052311 (2019).
- [8] S. T. Flammia and Y. K. Liu, Direct Fidelity Estimation from Few Pauli Measurements. *Phys. Rev. Lett.* 106, 230501 (2011).
- [9] E. Knill, D. Leibfried, R. Reichle, J. Britton, R. B. Blakestad, J. D. Jost, C. Langer, R. Ozeri, S. Seidelin and D. J. Wineland, Randomized benchmarking of quantum gates. *Phys. Rev. A* 77, 012307 (2008).
- [10] E. Magesan, J. M. Gambetta and J. Emerson, Scalable and Robust Randomized Benchmarking of Quantum Processes. *Phys. Rev. Lett.* 106, 180504 (2011).
- [11] J. J. Wallman and S. T. Flammia, Randomized benchmarking with confidence. *New J. Phys.* 16, 103032 (2014).
- [12] R. Harper and S. T. Flammia, Estimating the fidelity of T gates using standard interleaved randomized benchmarking. *Quantum Sci. Technol.* 2, 015008 (2017).
- [13] E. Onorati, A. H. Werner and J. Eisert, Randomized Benchmarking for Individual Quantum Gates. *Phys. Rev. Lett.* 123, 060501 (2019).
- [14] J. Helsen, X. Xue, L. M. K. Vandersypen and S. Wehner, A new class of efficient randomized benchmarking protocols. *npj Quantum Inf.* 5, 71 (2019).
- [15] H. J. Zhu and H. Y. Zhang, Efficient verification of quantum gates with local operations. *Phys. Rev. A* 101, 042316 (2020).
- [16] Y. C. Liu, J. W. Shang, X. D. Yu and X. D. Zhang, Efficient verification of quantum processes. *Phys. Rev. A* 101, 042315 (2020).
- [17] P. Zeng, Y. Zhou and Z. H. Liu, Quantum gate verification and its application in property testing. *Phys. Rev. Research* 2, 023306 (2020).
- [18] W. H. Zhang, X. Liu, P. Yin, X. X. Peng, G. C. Li, X. Y. Xu, S. Yu, Z. B. Hou, Y. J. Han, J. S. Xu, Z. Q. Zhou, G. Chen, C. F. Li and G. C. Guo, Classical communication enhanced quantum state verification. *npj Quantum Inf.* 6, 103 (2020).
- [19] S. Pallister, N. Linden and A. Montanaro, Optimal verification of entangled states with local measurements. *Phys. Rev. Lett.* 120, 170502 (2018).
- [20] H. Zhu and M. Hayashi, Efficient verification of hypergraph states. *Phys. Rev. Appl.* 12, 054047 (2019).
- [21] H. Zhu and M. Hayashi, Efficient verification of pure quantum states in the adversarial scenario. *Phys. Rev. Lett.* 123, 260504 (2019).
- [22] K. Wang and M. Hayashi, Optimal verification of two-qubit pure states. *Phys. Rev. A* 100, 032315 (2019).
- [23] X. D. Yu, J. Shang and O. Gühne, Optimal verification of general bipartite pure states. *npj Quantum Inf.* 5, 112 (2019).
- [24] Z. Li, Y. G. Han and H. Zhu, Efficient verification of bipartite pure states. *Phys. Rev. A* 100, 032316 (2019).
- [25] Y. C. Liu, X. D. Yu, J. Shang, H. Zhu and X. Zhang, Efficient verification of Dicke states. *Phys. Rev. Appl.* 12, 044020 (2019).
- [26] Z. Li, Y. G. Han and H. Zhu, Optimal verification of Greenberger-Horne-Zeilinger states. *Phys. Rev. Appl.* 13, 054002 (2020).
- [27] H. Zhu and M. Hayashi, Optimal verification and fidelity estimation of maximally entangled states. *Phys. Rev. A* 99, 052346 (2019).
- [28] H. J. Zhu and M. Hayashi, General framework for verifying pure quantum states in the adversarial scenario. *Phys. Rev. A* 100, 062335 (2019).
- [29] N. Dangniam, Y. G. Han and H. J. Zhu, Optimal verification of stabilizer states. *Phys. Rev. Research* 2, 043323 (2020).
- [30] Y. C. Liu, J. W. Shang, R. Han and X. D. Zhang, Universally Optimal Verification of Entangled States with Nondemolition Measurements. *Phys. Rev. Lett.* 126, 090504 (2021).
- [31] W. H. Zhang, C. Zhang, Z. Chen, X. X. Peng, X. Y. Xu, P. Yin, S. Yu, X. J. Ye, Y. J. Han, J. S. Xu, G. Chen, C. F. Li and G. C. Guo. Experimental optimal verification of entangled states using local measurements. *Phys. Rev. Lett.* 125, 030506 (2020).
- [32] X. H. Jiang, K. Wang, K. Y. Qian, Z. Z. Chen, Z. Y. Chen, L. L. Lu, L. J. Xia, F. M. Song, S. N. Zhu and X. S. Ma, Towards the standardization of quantum state verification using optimal strategies. *npj Quantum Inf.* 6, 90 (2020).
- [33] M. D. de Burgh, N. K. Langford, A. C. Doherty and A. Gilchrist, Choice of measurement sets in qubit tomography. *Phys. Rev. A* 78, 052122 (2008).
- [34] D. H. Mahler, Lee A. Rozema, A. Darabi, C. Ferrie, R. Blume-Kohout and A. M. Steinberg. Adaptive Quantum State Tomography Improves Accuracy Quadratically. *Phys. Rev. Lett.* 111, 183601 (2013).
- [35] K. S. Kravtsov, S. S. Straupe, I. V. Radchenko, N. M. T. Houlshby, F. Huszár and S. P. Kulik. Experimental adaptive Bayesian tomography. *Phys. Rev. A* 87, 062122 (2013).
- [36] A. Laing, T. Rudolph and Jeremy L. O'Brien, Experimental Quantum Process Discrimination. *Phys. Rev. Lett.* 102, 160502 (2009).
- [37] M. G. Díaz, K. Fang, X. Wang, M. Rosati, M. Skotiniotis, J. Calsamiglia and A. Winter. Using and reusing coherence to realize quantum processes. *Quantum* 2, 100 (2018).
- [38] O. Gühneab and G. Tóthc, Entanglement detection. *Phys. Rep.* 474, 1-6 (2009).
- [39] R. Okamoto, H. F. Hofmann, S. Takeuchi and K. Sasaki, Demonstration of an Optical Quantum Controlled-NOT Gate without Path Interference. *Phys. Rev. Lett.* 95, 210506 (2005).